Volume 19, Number 2, 2026. pp. 265-279

Jordan Journal of Physics

ARTICLE

Stellar Parameters and Evolutionary Pathways of the Subgiant System HIP 72217

Naufa Nazar[a], **Mashhoor A. Al-Wardat**[a,b], **Ahmad Abushattal**[c] and **Hassan B. Haboubi**[a]

[a] *Department of Applied Physics and Astronomy, College of Sciences, University of Sharjah, P.O. Box 27272 Sharjah, United Arab Emirates.*

[b] *Sharjah Academy for Astronomy, Space Sciences and Technology, University of Sharjah, P.O. Box 27272 Sharjah, United Arab Emirates.*

[c] *Department of Physics, Al-Hussein Bin Talal University, P.O. Box 20, Ma'an 71111, Jordan.*

DOI: **https://doi.org/10.47011/19.2.12**

Received on: 14/04/2025; *Accepted on: 07/05/2025*

Abstract: In this study, we applied Al-Wardat's method for analyzing stellar systems and variable stars to investigate the subgiant system HIP 72217, through which accurate stellar parameters were obtained, including stellar masses, effective temperatures (T_{eff}), and system age. For the primary component, we determined a mass of $M_A = 1.14 \pm 0.15\ M_\odot$ and effective temperature of $T_{eff,\ A} = 6125 \pm 50$ K, while for the secondary component, we obtained the values of $M_B = 1.12 \pm 0.14\ M_\odot$ and $T_{eff,\ B} = 5950 \pm 50$ K. The system's age was estimated to be 3.548 Gyr, which is consistent with the expected evolutionary stage of a subgiant binary system. The evolutionary timeline of HIP 72217 is clarified in this work, which also demonstrates the efficacy of Al-Wardat's method in determining the parameters of individual components within stellar systems. These findings contribute to a better understanding of the physical mechanisms that control subgiant binary evolution and their role in stellar evolution.

Keywords: Binary stars, Al-Wardat's method, Subgiant, Evolutionary tracks, Isochrones.

Introduction

The study of stellar star systems leads to an enhanced understanding of stellar evolution because researchers can directly measure essential stellar properties, including mass, radius, and luminosity [1–5]. Subgiant stars serve as essential research objects to study the main-sequence to giant-phase transition because they reveal information about core hydrogen exhaustion and shell hydrogen-burning processes [6]. Studying subgiants in binary or triple systems provides valuable insights into stellar evolution, as the evolutionary pathways of subgiants are directly influenced by dynamical interactions and mass transfer between the stellar components [1]. The subgiant system HIP 72217 provides researchers with an exceptional chance to study these phenomena extensively.

Binary systems fall into three main types: astrometric binaries, spectroscopic binaries, and eclipse binaries. One technique alone cannot determine an individual system mass. For the last fifty years, scientists worldwide have used speckle interferometry to observe binary stars effectively and accurately [7–10]. Due to the processes involved in star formation, multiple-star systems are more likely to host massive exoplanets. A binary star's physical properties determine the habitability and stability of an exoplanet, both of which are essential parameters in exoplanet studies. This study mainly focuses on the parameters of individual masses, semi-major axes, luminosities, and temperatures [11–16]. Al-Wardat's method for analyzing stellar systems is a useful tool for determining accurate

Corresponding Author: Mashhoor A. Al-Wardat **Email**: malwardat@sharjah.ac.ae

stellar parameters. This method combines photometry and model atmospheres to create synthetic spectral energy distribution (SED) and to identify sub-components or sub-systems of the components of the stellar system. As mentioned earlier, Al-Wardat's method enables the highly accurate determination of the masses, radii, effective temperatures, and luminosities when the observed data is compared to the theoretical models (see: [17–26]). HIP 72217 is a triple star system located in the Libra constellation. It is composed of a close inner binary pair (HIP 72217 A and B) with a separation of 0.182 mas orbited by a more distant companion (HIP 72217 C) with a separation of 6.923 mas. Applying this to a system such as HIP 72217 helps to gain insight into the physical characteristics and possible evolutionary stages of stellar systems, especially those in the subgiant category.

Although the method provides an effective analysis of the stellar parameters, it does have certain limitations. The main drawback of this method stems from its requirement of theoretical stellar atmosphere models such as Kurucz or PHOENIX which depend on assumptions regarding static, plane-parallel, and local thermodynamic equilibrium (LTE) conditions. The stellar atmosphere models used in this method do not provide a comprehensive simulation of non-LTE phenomena, stellar activity effects, or convective overshooting, all of which are particularly important in evolved or active stars. The method requires complete knowledge of stellar components because any unresolved objects or mishandling of interstellar effects would result in systematic measurement errors. The precision of synthetic spectral energy distribution (SED) fitting depends largely on the initial values of metallicity and interstellar reddening because incorrect estimates from these parameters affect the determination of temperature, luminosity, and radius. Al-Wardat's method needs external verification through independent methods such as interferometry, spectroscopy, and asteroseismology to eliminate parameter uncertainty and validate results.

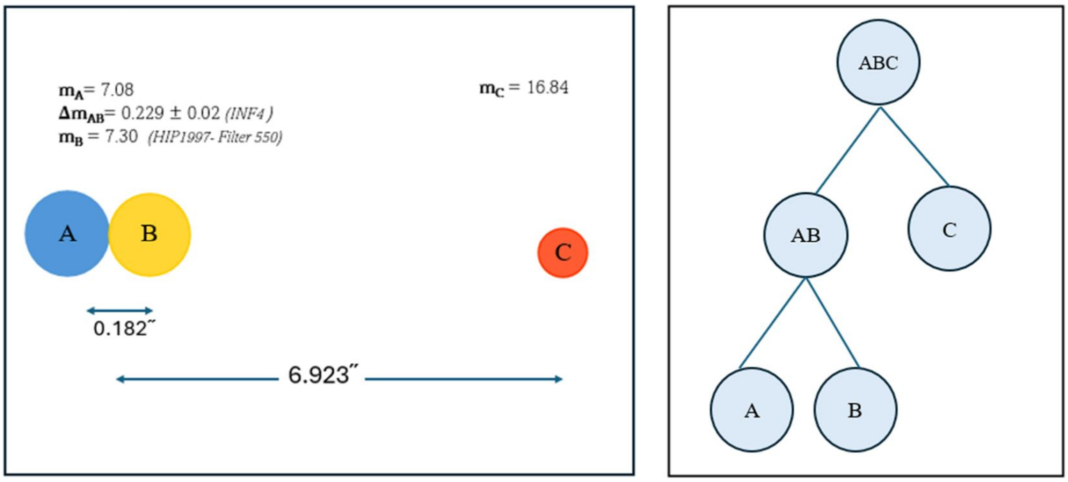

FIG. 1. **Left:** Pictorial representation of the three components A, B and C of the system HIP 72217 with their magnitudes (mvA = 7.08, mvB = 7.30, mvC =16.84) and magnitude differences [27]. Their separation in mas is also denoted in the picture. **Right:** Hierarchical chart showing the combinations of the three components.

2. Observational Data

The study of the HIP 72217 system involved gathering observational data from multiple sources to analyze its stellar components. Table 1 summarizes the observational data, including B- and V-band apparent magnitudes, spectral classifications, the m_V magnitude difference, and Hipparcos parallax measurements.

TABLE 1. Observational data for HIP 72217

	HIP 72217 HD 129980	Source
α_{2000}	14h 46m 10.89	Simbad [28]
δ_{2000}	−21° 10′ 33.46	Simbad [28]
Sp. Type	G1V	Simbad [28]
$(\Delta m_v)_{A,B}$	0.229 ± 0.02	INF4 [29]
$(\Delta m_v)_{AB,C}$	10.41 ± 0.10	UMSC [30]
A_v	0.005	G-Tomo [31]
V_J	6.43 ± 0.01	Tycho [32]
B_J	7.04 ± 0.02	Tycho [32]
$(B - V)_J$	0.603 ± 0.004	Tycho [32]
π_{Hip}	23.64 ± 1.07	ESA1997 [33]
π_{Hip}	24.24 ± 0.63	VNHR2007 [34]

3. Spectrophotometric Analysis of the System

We applied Al-Wardat's method for analyzing stellar systems to study the target system. This technique combines theoretical stellar atmospheres with photometric observations to derive precise physical parameters [19, 35, and 36]. The analysis first considers the magnitude difference (Δm) between the components and the system's total visual magnitude (m_V). The spectral energy distribution (SED) is then constructed using the effective temperature and surface gravity (log g) [37–39], where the flux ratio of the components is given by:

$$\frac{f1}{f2} = 2.512^{-\Delta m} \quad (1)$$

$$m_v = -2.5\log(f_1 + f_2) \quad (2)$$

From these, we determine the apparent magnitudes of both stars:

$$m_v^{(A)} = m_v + 2.5\log\left(1 + 10^{-0.4\Delta m}\right) \quad (3)$$

$$m_v^{(B)} = m_v^{(A)} + \Delta m \quad (4)$$

The uncertainties in these magnitudes are calculated as:

$$\sigma^2_{m_v^{(A)}} = \sigma^2_{m_v} + \left(\frac{10^{-0.4\Delta m}}{1+10^{-0.4\Delta m}}\right)^2 \sigma^2_{\Delta m} \quad (5)$$

$$\sigma^2_{m_v^{(B)}} = \sigma^2_{m_v^{(A)}} + \sigma^2_{\Delta m} \quad (6)$$

Next, the absolute magnitudes (Mv) are derived using the distance (d in parsecs) and extinction (Av):

$$M_v = m_v + 5 - f\log(d) - A_v \quad (7)$$

The errors in absolute magnitudes are:

$$\sigma^2_{M_v^{(A)}} = \sigma^2_{m_v^{(A)}} + (\ln(0.2\pi))^2\sigma^2_\pi \quad (8)$$

$$\sigma^2_{M_v^{(B)}} = \sigma^2_{m_v^{(B)}} + (\ln(0.2\pi))^2\sigma^2_\pi \quad (9)$$

Using these, we estimate the effective temperature and bolometric correction (BC) from [40, 41], before computing the bolometric magnitude:

$$M_{bol} = M_v + BC \quad (10)$$

The stellar luminosity follows from:

$$M_{bol} - M_{\odot,bol} = -2.5\log\left(\frac{L}{L_\odot}\right) \quad (11)$$

The radii are then determined via:

$$\log\left(\frac{R}{R_\odot}\right) = 0.5\log\left(\frac{L}{L_\odot}\right) - 2\log\left(\frac{T}{T_\odot}\right) \quad (12)$$

Masses are estimated using empirical relations from [40], and the surface gravity is found using:

$$\log(g) = \log\left(\frac{M}{M_\odot}\right) - 2\log\left(\frac{R}{R_\odot}\right) + 4.43 \quad (13)$$

$$m_p = -2.5\log\frac{\int P_p(\lambda)F_{\lambda,s}(\lambda)d\lambda}{\int P_p(\lambda)F_{\lambda,r}(\lambda)d\lambda} + ZP_p \quad (14)$$

where:

- mp: synthetic magnitude in passband p,
- Pp(λ): normalized sensitivity function of passband p,
- Fλ,s(λ): synthetic SED of the star,
- Fλ,r(λ): Vega's reference SED,
- ZPp: Vega-based zero-point calibration [34].

Color indices are computed, and SED magnitudes are estimated using Al-Wardat's synthetic photometry method. To achieve the best fit between synthetic and observational visual magnitudes, color indices, and magnitude differences, an iterative method is employed [17, 42, 43].

In the sub-Fig. 3(a), the Eigenvalue Rank on the X-axis depicts the PCs, while the percentage of total variance computed for each PC is shown on the Y-axis. The scatter plots (c-d) illustrate the displacement distribution of P-atoms between two different principal components (PCs). The color gradient from red through blue to white represents the extent of deviations experienced by the P- atoms as a function of time during the 100 ns simulation.

4. Orbital Analysis

The orbital solution for the HIP 72217 system was derived using Tokovinin's ORBITX code [44]. This method requires the following input parameters:

- Right ascension (RA) in the format HH.MMSS.
- Declination (Dec) in the format DD.MMSS.
- Orbital period P (initial value in years).
- Epoch of periastron passage T (in years).
- Eccentricity e.
- Semi-major axis a (in arcseconds).
- Position angle of the line of nodes Ω (in degrees).
- Longitude of periastron ω (in degrees).
- Inclination i (in degrees).
- Semi-amplitudes of radial velocities K1 and K2 (in km/s) for the primary and secondary components, respectively.
- Systemic velocity V0 (in km/s).

These parameters were sourced from the Sixth Catalog of Orbits of Binary Stars [45].

Additionally, angular separations ρ (in arcseconds) and position angles θ (in degrees) were obtained from the Fourth Catalog of Interferometric Measurements of Binary Stars [29]. The dynamical mass of the system was calculated using Kepler's Third Law for binary stars:

$$M_{dyn} = M_A + M_B = \left(\frac{a^3}{\pi^3 P^2}\right) M_{\odot}, \tag{15}$$

where π is the parallax, a is the semi-major axis of the relative orbit of the binary system in arcseconds, and P is the orbital period in years.

The formal error in the mass was determined using:

$$\frac{\sigma M}{M} = \sqrt{9\left(\frac{\sigma_\pi}{\pi}\right)^2 + 9\left(\frac{\sigma_a}{a}\right)^2 + 4\left(\frac{\sigma_P}{P}\right)^2} \tag{16}$$

5. Results

5.1. Spectrophotometric Analysis

Figure 2 shows the observed photometric data points from various bands plotted against the synthetic SED generated for the best-fitting stellar parameters of the two components.

The individual contributions of Component A and Component B to the total flux are also displayed, highlighting their relative influence on the combined spectrum. The agreement between the observed photometric data points (colored markers) and the model SED (black curve) demonstrates the robustness of the derived stellar parameters, particularly the effective temperatures (T_{eff},A = 6125 K, T_{eff},B = 5950 K) and surface gravities (log gA = 4.14, log gB = 4.20).

The synthetic magnitudes derived from this SED fitting align well with the observed magnitudes, with minimal deviations in the Gaia and Johnson-Cousins photometric bands. This provides additional validation of the accuracy of the modeled stellar properties.

Using the SEDs and Eq. (14), we calculated the synthetic magnitudes of the total system and the components, as listed in Table 2. The magnitude difference Δm_v between the two components is also presented in Table 3, where the synthetic values are compared with the observed values. The obtained results are consistent with the observed values in Table 1. This strong correlation can be seen to confirm our approach because the parameters estimated in the analysis are consistent with theoretical expectations and with the observed values of the star. This correspondence further supports the validity of the method and confirms the credibility of the determined stellar parameters seen in Table 4. We included in our analysis of the binary system AB a third component C, which is known to have a mass of 0.17 $M_{\odot}$. Nevertheless, our study was mostly based on the AB components, since there were no observational parameters, such as the B − V color index. Although Component C was taken into account in the overall system dynamics, we were unable to carry out a detailed analysis of it due to lack of data. However, we were able to estimate its effective temperature (T_{eff}) of 3250 K and radius of 0.28 $R_{\odot}$, and a synthetic magnitude that agrees with the observed value of 16.84. Using this estimation and the observed Δm_v (AB, C) we were able to conduct some analyses for the component.

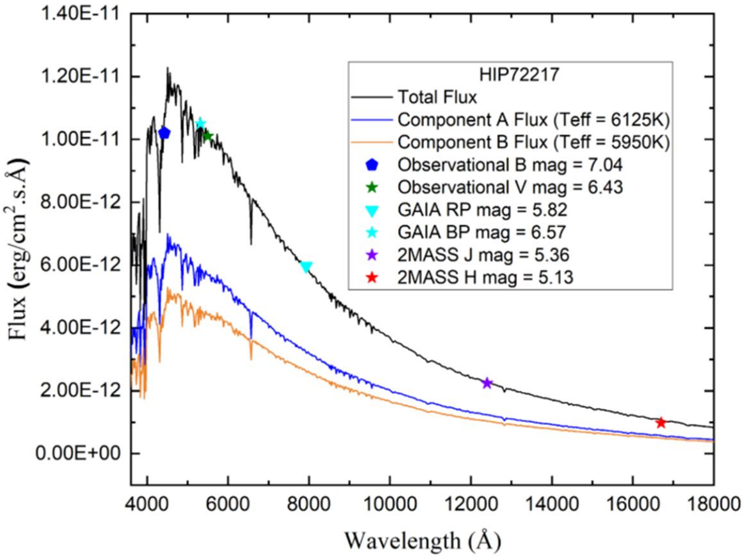

FIG. 2. Spectral energy distribution (SED) of HIP 72217, showing the combined synthetic SED of the binary system along with individual flux contributions from each component.

* Observed magnitudes from Gaia [46], 2MASS [32] and Tycho [47] are overlaid for comparison.

TABLE 2. Synthetic (Syn) magnitudes of components A, B, and C, and the total flux compared with available observed (Obs) magnitudes.

Filter	Syn Total ($\sigma = 0.05$)	Obs Total	Syn Star A ($\sigma = 0.02$)	Syn Star B ($\sigma = 0.04$)	Syn Star C
B Johnson	7.04	7.04 ± 0.02	7.64	7.96	18.7
V Johnson	6.42	6.43 ± 0.01	7.06	7.33	16.82
R Cousins	5.81	–	6.44	6.69	15.3
I Cousins	5.43	–	6.08	6.31	14.19
J 2MASS	5.37	5.36 ± 0.027	6.03	6.22	12.55
H 2MASS	5.04	5.10 ± 0.04	5.67	5.84	11.38
G Gaia	6.31	6.30 ± 0.001	6.95	7.20	15.44
B_p Gaia	6.64	6.57 ± 0.001	7.26	7.55	17.31
R_p Gaia	5.85	5.82 ± 0.001	6.49	6.72	14.29
B − V	0.602	0.603	0.583	0.627	1.877
$B_p - R_p$	0.797	0.754	0.769	0.832	3.06

TABLE 3. Comparison of synthetic and observed ΔmV (A, B) values.

Type	Δm_v	Source
Synthetic	0.26 ± 0.05	(This Work)
Observed 1	0.20 ± 0.05	Tok2010 S [49]
Observed 2	0.20 ± 0.04	Tok2012d St [50]
Observed 3	0.30 ± 0.06	Tok2015c St [51]
Observed 4	0.30 ± 0.05	Tok2016a St [52]

TABLE 4. Parameters for Components A, B, and C of HIP 72217.

Parameters	Units	Component A	Component B	Component C
$M_v \pm \sigma M_v$	(mag)	4.03 ± 0.02	4.29 ± 0.03	13.79 ± 0.2
$M_{(bol)} \pm \sigma M_{(bol)}$	(mag)	3.659 ± 0.01	3.888 ± 0.02	10.01 ± 0.1
$L \pm \sigma L$	(L⊙)	2.73 ± 0.19	2.21 ± 0.14	0.007 ± 0.0002
$T_{eff} \pm \sigma T_{eff}$	(K)	6125 ± 50	5950 ± 50	3250 ± 50
$R \pm \sigma R$	(R⊙)	1.47 ± 0.04	1.39 ± 0.03	0.28 ± 0.01
$M \pm \sigma M$	(M⊙)	1.14 ± 0.15	1.12 ± 0.14	0.17 ± 0.01
$\log(g) \pm \sigma\log(g)$	(cm s^{-2})	4.14 ± 0.11	4.20 ± 0.12	4.76 ± 0.17

The positions of the components of HIP 72217 on the Hertzsprung-Russell diagram (HRD) are shown in Fig. 3 with the evolutionary tracks corresponding to the metallicity Z = 0.03. The key is as follows: blue stars refer to the primary star, while magenta stars refer to the secondary star.

The evolutionary tracks, which are derived from model stellar evolution, give an approximate age of the system by identifying the position of each star on the corresponding track. When compared with the nearest isochrone (dotted cyan line), the age of the system is estimated to be 3.548 Gyr.

As is evident from their positions on the diagram, Components A and B are somewhat post-MS and possess some features of a subgiant. The estimated masses of the components based on the tracks are MA ≈ 1.14M⊙ and MB ≈ 1.12M⊙, which confirms the classification of the primary and secondary components as subgiants.

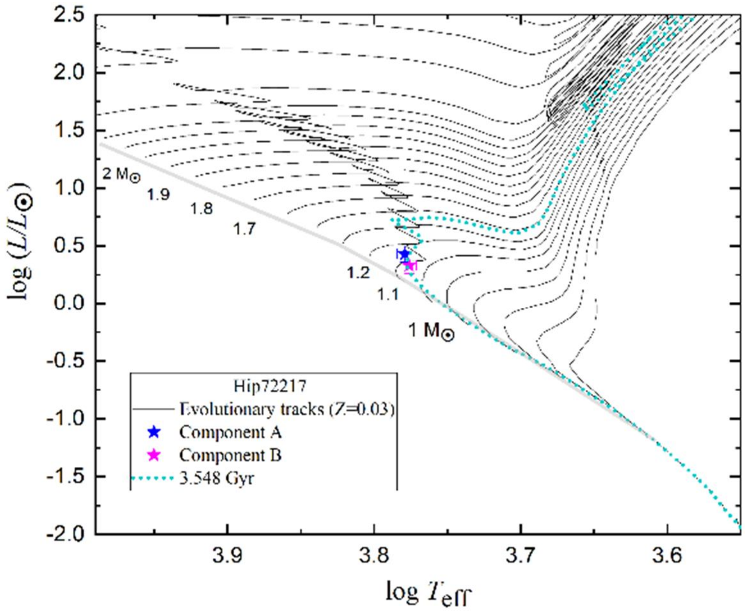

FIG. 3. Component A and B of HIP 72217 placed on the Evolutionary Track and Isochrone of Z = 0.03 taken from Girardi [51]. The HR diagram shows a plot of log of effective temperature plotted against log(L/L⊙), the logarithm of the ratio of the stellar luminosity to the Solar Luminosity.

The results obtained from both the evolutionary tracks and SED fitting methods converge on a self-consistent model for the system, reinforcing the classification of HIP 72217s AB binary sub-system as subgiants. The mass and age estimations from the HRD align well with those inferred.

The derived age of 3.548 ± 0.3 Gyr for this system provides significant value when researchers compare it to other well-studied subgiant binaries. Theoretical predictions match the observed age range for stars in the solar-type mass range from 1.1 M⊙ to 1.2 M⊙ that move off the main sequence. Research shows that subgiant binaries with matching mass and metallicity characteristics normally have ages between 2.5 and 6.5 Gyr [1]. Asteroseismic and evolutionary modeling [52] determined that the α Centauri system, with 1.10 M⊙ and 0.91 M⊙ components, has an age of 6.5 ± 1.0 Gyr. The evolutionary stage of HIP 72217 can be determined as being early subgiant, based on its proximity to the 3.5 Gyr isochrone in the Hertzsprung–Russell diagram using Z = 0.03 [53]. This suggests that both components A and B have only recently departed from the main sequence, marking the beginning of the hydrogen shell-burning phase. Our age determination through stellar evolutionary tracks and the subgiant system age distribution in published literature shows good agreement, which validates both the modeling approaches and the derived stellar parameters.

5.2. Orbital Solution

The HIP 72217 system's orbital solution was computed using Tokovinin's ORBITX code. The refined orbital elements and data from Mason (2010) are shown in Table 5. The Table contains the final orbital elements derived from HIP 72217. The updated observational data combined with improved fitting methods delivers more precise dynamical mass estimates that are essential for stellar characterization. The Mason (2010) [54] study provided initial orbital parameters for the binary star system HIP 72217, but the results of this work indicate a more rigorous fit because they are based on newer observational data points.

The total dynamical mass of the system was determined using Kepler's Third Law 15 with a newly suggested parallax of $\pi = 25.65$ mas. This adjustment, based on the system's observed properties, yielded a dynamical mass of Mdyn = 2.26 $M_{\odot}$ which is in excellent agreement with the total mass obtained from Al-Wardat's method (MA + MB = 2.26 ±0.29 $M_{\odot}$). The consistency between these independent methods validates both the orbital solution and the stellar parameter determination, while resolving discrepancies in previous mass estimates.

The residuals of the orbital fit demonstrate high precision (RMS θ = 2.12°, RMS ρ = 0.0127 arcsec). Fig. 4 shows the computed orbit's excellent agreement with historical measurements from Table 6, further confirming the solution.

TABLE 5. Observational points and measurements with sources.

Date	θ (deg)	ρ (deg)	Source
1951.510	151.2	0.312	Fin1951b J
1952.500	165.2	0.260	Fin1953d J
1953.560	178.8	0.204	Fin1954c J
1954.580	200.3	0.210	Fin1954c J
1966.620	174.6	0.200	Fin1967a J
1978.316	160.1	0.241	McA1984b Sc
1980.481	195.2	0.175	McA1983 Sc
1984.375	94.8	0.188	McA1987b Sc
1984.378	94.5	0.190	McA1987b Sc
1985.514	111.8	0.240	McA1987a Sc
1986.407	118.5	0.258	McA1989 Sc
1987.272	126.6	0.280	McA1989 Sc
1989.230	141.4	0.279	McA1990 Sc
1989.303	142.4	0.283	McA1990 Sc
1990.273	150.6	0.271	Hrt1992b Sc
1990.341	150.6	0.263	Hrt1993 Sc
1991.250	160.0	0.239	HIP1997a Ih
1993.095	185.7	0.168	Hrt2000a Sc
1996.184	63.6	0.108	Hrt2000a Sc
2001.498	137.2	0.290	Hor2008 S
2001.498	137.4	0.291	Hor2008 S
2006.189	188.6	0.158	Msn2010c Su
2008.536	12.6	0.066	Tok2010 S
2008.542	12.9	0.066	Tok2010 S
2008.547	13.9	0.067	Tok2010 S
2009.262	70.0	0.119	Tok2010 S
2009.652	77.0	0.142	Rho2010 O
2010.587	94.3	0.224	Msn2011d Su
2011.289	110.3	0.238	Tok2012d St
2014.303	136.0	0.290	Tok2015c St
2015.335	143.4	0.284	Tok2016a St
2019.210	191.4	0.156	Tok2020
2022.197	70.8	0.120	Msn2023
2023.105	95.8	0.184	Tok2024

TABLE 6. Refined orbital elements and residuals for HIP 72217 (with comparison to Mason, 2010).

Parameter	Unit	This Work	Mason (2010) [54]
Period *P*	yr	12.917 ± 0.0012	12.929 ± 0.021
Epoch *T*	yr	1995.2607 ± 0.0022	1995.2490 ± 0.0550
Eccentricity *e*	–	0.6319 ± 0.0012	0.6428 ± 0.0051
Semi-major axis *a*	arcsec	0.1854 ± 0.0003	0.1814 ± 0.0021
Ω	deg	277.42 ± 0.96	281.9 ± 4.10
ω	deg	44.42 ± 0.91	39.5 ± 4.70
Inclination *i*	deg	25.29 ± 0.31	25.90 ± 2.60
K_1	km/s	7.06 ± 0.00	7.06 ± 0.00
K_2	km/s	7.32 ± 0.00	7.32 ± 0.00
V_0	km/s	−2.00 ± 0.00	−2.00 ± 0.00
RMS θ	deg	2.12	–
RMS ρ	arcsec	0.0127	–
χ^2	–	6941.74	–

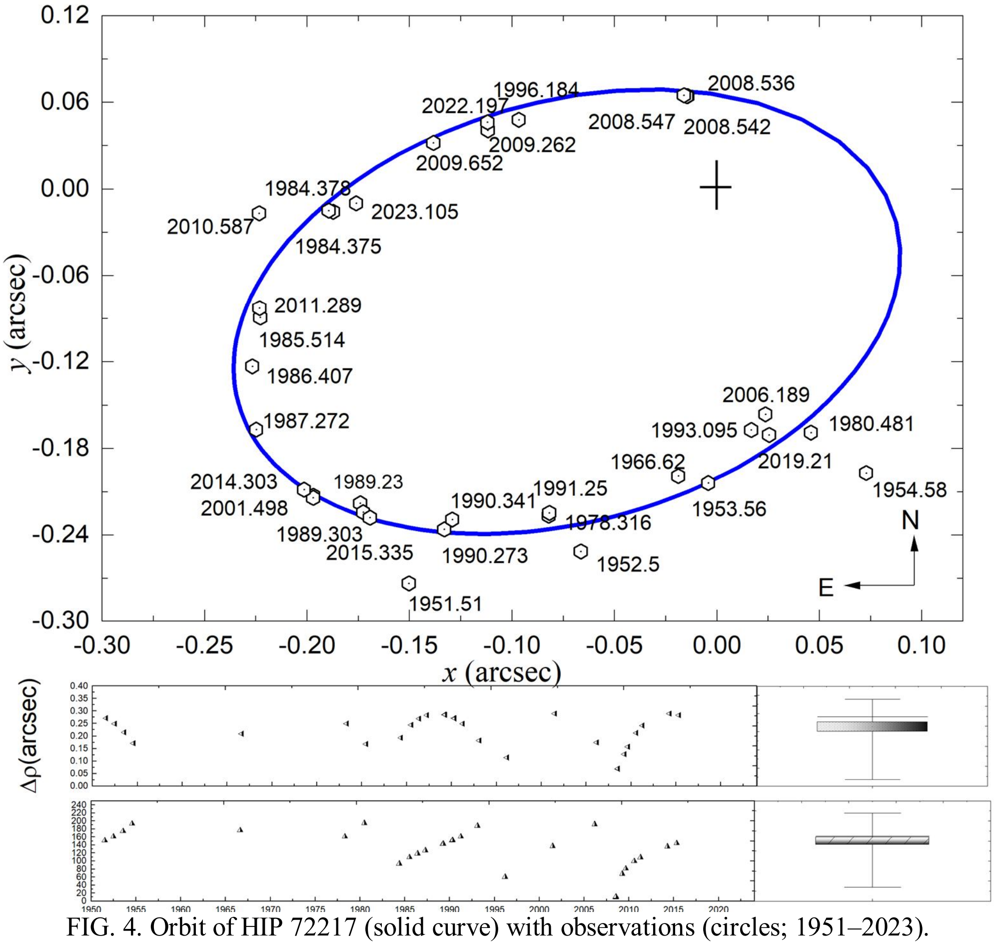

FIG. 4. Orbit of HIP 72217 (solid curve) with observations (circles; 1951–2023).

* The bottom left panel displays fit residuals that indicate the differences between observed and modeled angular separation (Δρ) and position angle (Δθ) measurements of the orbit. The bottom right panel shows a box plot that summarizes data distribution by displaying minimum and maximum values, first (Q1) and third (Q3) quartiles, median, and any detected outliers.

6. Stability and Habitability of HD 72217

6.1. Stability Analysis

The analysis of orbital stability is inherently complex due to numerous influencing factors, including initial conditions, mathematical frameworks, and physical constants [55]. In binary star systems, an orbit is typically considered stable if the primary orbital parameters- eccentricity, semimajor axis, and inclination- remain relatively constant over long timescales.

Habitability, as defined by [56], refers to the ability of an environment to support the metabolic processes of at least one known organism, thus allowing its survival, growth, and reproduction.

This study employs the empirical stability equations derived by Holman and Wiegert [58] to delineate the stable orbital zones around the HD 72217 binary system. Two orbital types are examined: circumstellar (S-type), where a planet orbits a single star, and circumbinary (P-type), where a planet orbits both stars. Critical stability boundaries for these scenarios depend primarily on the binary's semi-major axis, mass ratio, and eccentricity.

To assess orbital stability within the HD 72217 system, we applied the empirical expressions of Holman and Wiegert [57] for S-type and P-type orbits. The critical semi-major axis for S-type orbits is given by:

as = a [(0.464 ± 0.006) + (−0.380 ± 0.010) μ + (−0.631 ± 0.034) e + (0.586 ± 0.061) μe + (0.150 ± 0.041) e^2 + (−0.198 ± 0.047) μe^2]

For P-type orbits, the critical semi-major axis is:

ap = a [(1.60 ± 0.04) + (4.12 ± 0.09) μ + (5.10 ± 0.05) e + (−4.27 ± 0.17) μe + (−2.22 ± 0.11) e^2 + (−5.09 ± 0.11) μ^2+ (4.61 ± 0.36)$\mu^2 e^2$]

Here, a is the binary semi-major axis, e is the binary eccentricity, and μ = M1 / (M1 +M2) is the mass ratio of the primary to the total mass.

6.2. Habitable Zone Calculation

Habitable zone (HZ) distances around stars are derived following the approach outlined by Kopparapu et al. (2013) [59]. The analysis begins with calculating the effective stellar flux, adjusted for differences in stellar temperature relative to the Sun. The effective flux is calculated via:

$$S_{eff} = S_{eff\odot} + a\Delta T + b(\Delta T)^2 + c(\Delta T)^4 \quad (17)$$

where ΔT = Tstar − $T_\odot$, and a, b, c, and d are empirically determined coefficients. The corresponding habitable zone distance is:

$$d_{HZ} = \sqrt{\frac{\frac{L}{L_\odot}}{S_{eff}}} \quad (18)$$

where $L/L_\odot$ denotes the star's luminosity relative to the Sun. Each star within the HD 72217 system has unique habitable zones determined individually. Table 7 summarizes the stellar flux and resulting HZ distances for different climate scenarios.

6.3. Habitable Zone Distances

To define HZ for HD 72217, Kopparapu et al. (2013) [59] proposed a classification of climate scenarios. According to different planetary climate models, these scenarios represent theoretical thresholds that constrain the inner and outer edges of the HZ. According to the Recent Venus scenario, Venus is believed to have lost its surface water as a result of intense solar irradiation near the inner edge of the habitable zone. A planet reaches the Runaway Greenhouse Limit when greenhouse warming becomes uncontrollable, ultimately rendering the planet uninhabitable. Water vapor saturation in the atmosphere in the Moist Greenhouse scenario could lead to hydrogen escape into space, resulting in increased greenhouse gas concentrations. Water can still exist at a distance of the Maximum Greenhouse limit even after carbon dioxide-induced warming has reached its maximum. In addition, the Early Mars scenario posits that Mars may have had liquid water under past solar conditions, which represents the most distant boundary of the HZ. Based on these established scenarios, we can calculate the stellar flux (S_{eff}) and HZ distance for both the primary and secondary stars. Table 8 provides stability limits and HZ ranges for both circumstellar and circumbinary orbits in the HD 72217 system.

Figure 5 illustrates the overall habitability and stability regions for the complete HD 72217 binary system, while Figs. 6 and 7 focus more specifically on the regions around the primary and secondary stars, respectively. The shaded areas denote habitable zones, and dashed lines delineate stability boundaries where planetary orbits remain viable over long periods.

TABLE 7. Summary of the effective stellar fluxes (Seff) and the corresponding inner and outer boundaries of the habitable zone under five climate scenarios: Recent Venus, Runaway Greenhouse, Moist Greenhouse, Maximum Greenhouse, and Early Mars. S_{eff} values and resulting HZ distances (in AU) are provided separately for both the primary and secondary components.

Scenario	S_{eff} 1	a	b	c	d	S_{eff} 2	Primary HZ (AU)	Seff,2	Secondary HZ (AU)
Recent Venus	1.7753	0.000143	2.9875e-08	−7.5702e-12	−1.1635e-15	1.842718	1.223160	1.799685	1.108148
Runaway Greenhouse	1.0512	0.000132	1.5418e-08	−7.9895e-12	−1.8328e-15	1.098366	1.576550	1.074116	1.434101
Moist Greenhouse	1.0140	0.000082	1.7063e-09	−4.3241e-12	−6.6462e-16	1.042228	1.618452	1.027929	1.466272
Maximum Greenhouse	0.3438	0.000059	1.6558e-09	−3.0015e-12	−5.2983e-16	0.364201	2.578560	0.355853	2.499107
Early Mars	0.3179	0.000055	1.5313e-09	−2.7786e-12	−4.8979e-16	0.336768	2.847186	0.327197	2.598910

TABLE 8. Stability distances and habitable zone ranges for the HD 72217 system.

Parameter	Value (AU)
S-type stability distance (nominal)	0.062
S-type stability distance (min)	0.003
S-type stability distance (max)	0.067
P-type stability distance (nominal)	2.946
P-type stability distance (min)	2.734
P-type stability distance (max)	2.966
HD 72217 A HZ range	1.223 – 2.847
HD 72217 B HZ range	1.108 – 2.599

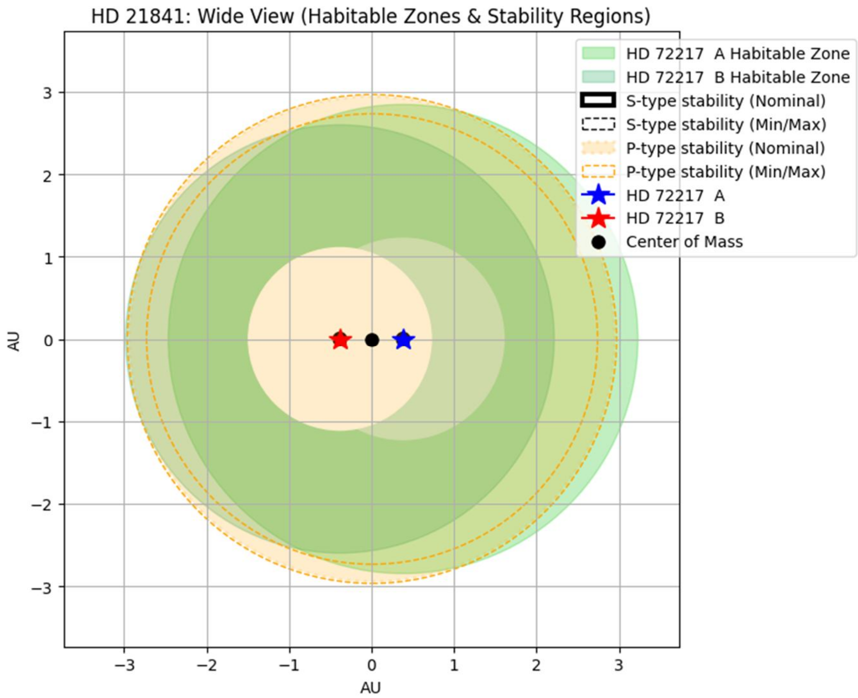

FIG. 5. Habitable zones (green area) and stability boundaries (dashed line) for the entire HD72217 binary system.

Using analytical models, this Figure illustrates the potential habitable zones (green shaded areas) for HD 72217. It is entirely based on calculated criteria (Holman & Wiegert, 1999 [57]; Kopparapu et al., 2013 [58]), without any direct observations. In this Figure, no residuals are plotted since no empirical data are used. Within the system, it provides a conceptual map for evaluating potential planetary stability and habitability.

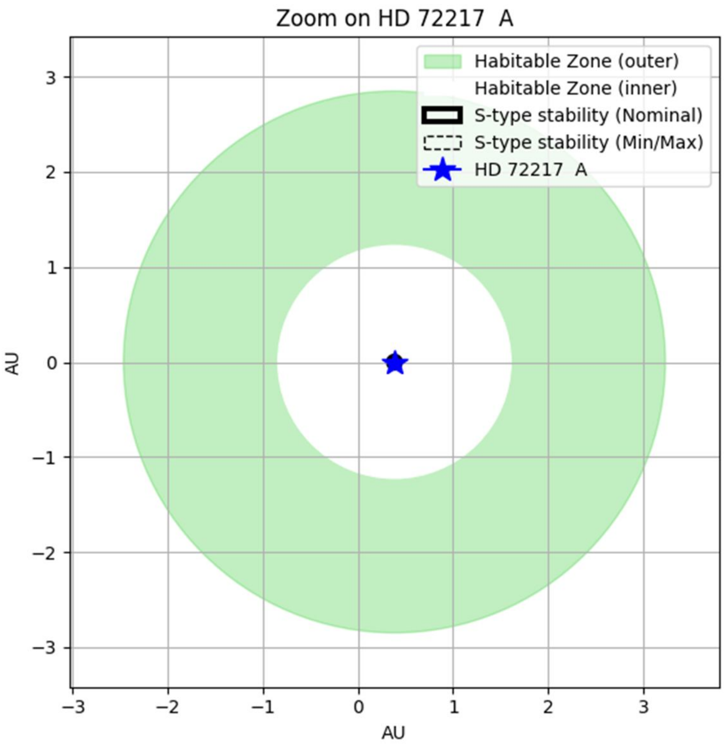

FIG. 6. Habitability and stability zones around the primary star HD 72217 A.

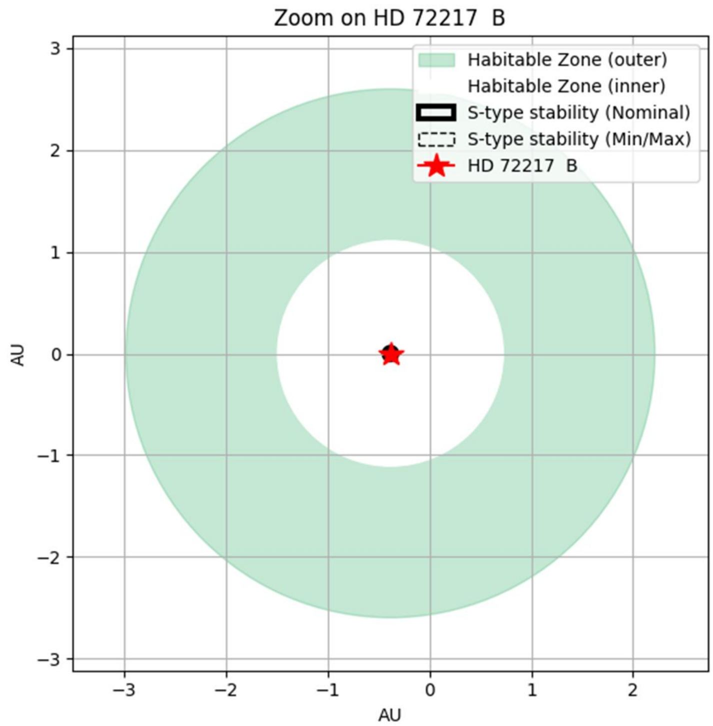

FIG. 7. Habitability and stability zones around the secondary star HD 72217 B.

This detailed analysis is crucial for evaluating the potential habitability of planets within binary star systems, highlighting the strong influence of stellar properties on the extent and position of habitable zones.

Although our calculations establish theoretical limits on stability and habitability in the HD 72217 system, detecting planets in similar close binary systems remains observationally challenging. Small stellar separations (approximately 0.182 mas in the case of HIP 72217 AB) complicate radial velocity measurements because combined gravitational perturbations and stellar activity effects can suppress subtle planetary signals. Even with direct-imaging techniques, the high brightness contrast and small angular separation between the stars and potential planets present major observational limitations. These challenges may be mitigated through advanced techniques such as interferometry and high-contrast adaptive optics implemented in specialized, long-term observational campaigns using state-of-the-art telescopes.

7. Conclusion

In this work, we used Al-Wardat's method for analyzing stellar systems and Tokovinin's dynamical method to study the triple system HIP 72217 and determine the stellar parameters of its components. We found that two of the three components (A and B) of the system are subgiant stars, while the third component (C) is a red dwarf main sequence star. The first component has a mass of MA = 1.14 ± 0.15 $M_\odot$ and effective temperature T_{eff},A = 6125 ± 50 K, and the second component has a mass of MB = 1.12 ± 0.14 $M_\odot$ and effective temperature T_{eff},B = 5950 ± 50 K. Component C has been confirmed to have a mass of MA = 0.17 ± 0.04 $M_\odot$ with an effective temperature of T_{eff}, C = 3250 ± 50 K.

The derived age of the AB system, 3.548 Gyr, is consistent with theoretical expectations for stars with masses of 1.1–1.2 $M_\odot$ evolving from the main sequence toward the subgiant phase. These results agree with the evolutionary models presented in [55] for Z = 0.03, which predict subgiant evolution for masses around this age. Systems with similar masses were reported to have subgiant binary ages of 2.5−4.5 Gyr in comparative studies such as [1] and [17], which support the validity of our result. Meanwhile, the age of the component C cannot be empirically stated since it lies at the bottom of the main sequence. The orbital solution for HIP 72217, derived using Tokovinin's ORBITX code, demonstrates excellent consistency between dynamical and theoretical mass estimates. A revised parallax of π = 25.65 mas yields a dynamical mass of 2.26 $M_\odot$, in precise agreement with Al-Wardat's method (2.26 ± 0.29 $M_{\odot}$), thus resolving prior discrepancies. The fit shows high precision, with low residuals (RMS θ = 2.12°, RMS ρ = 0.0127″), and the computed orbit closely matches historical observations. This robust agreement validates both the orbital parameters and the system's stellar properties.

This work includes a comprehensive analysis of the orbital stability of HIP 72217 as well as the potential habitability of the system. We computed the critical semimajor axes for circumstellar (S-type) and circumbinary (P-type) orbital stability using the empirical criteria developed by Holman and Wiegert [57]. According to the results, S-type stable zones lie between 0.003 and 0.067 AU, with a nominal boundary at 0.062 AU, while P-type stable zones lie beyond 2.734 AU, peaking at 2.946 AU. Based on Kopparapu et al. [58], we used a stellar flux model to assess habitability, considering variations in effective temperature and luminosity. Therefore, the habitable zone of the primary star ranges from 1.223 to 2.847 AU, while the habitable zone of the secondary extends from 1.108 to 2.599 AU. These results show that the two components comprise distinct but overlapping habitable zones, collectively defining an area suitable for circumbinary life. Consequently, stellar characteristics are crucial to the development of a life-friendly environment. Such complex binary configurations require future observational campaigns and refined dynamical models to identify stable, life-sustaining exoplanets.

This analysis provides a valuable benchmark for testing and refining existing evolutionary models, particularly in the subgiant phase—a critical transitional stage between the main sequence and the red-giant branch. The results, consistent with theoretical isochrones, strengthen the reliability of current evolutionary tracks. These findings enhance our understanding of internal stellar processes such as hydrogen-shell burning and envelope expansion, and they contribute to improving the precision of stellar-population synthesis models. Ultimately, the detailed study of subgiant binaries like HD 72217 bridges the gap between observational astrophysics and theoretical stellar physics, advancing both fields.

8. Acknowledgement

This study employed a range of resources and tools, including SAO/NASA, the SIMBAD database, the Fourth Catalog of Interferometric Measurements of Binary Stars, IPAC data systems. Furthermore, it utilized the MCMC ORBIT code and codes of Al-Wardat's method for analyzing stellar systems and variable stars, including its sub-codes for spectrophotometric calculations and its technique for estimating parallaxes, masses and metallicities.

References

[1] Torres, G., Andersen, J., and Gim´enez, A., The Astronomy and Astrophysics Review, 18 (1–2) (2009) 67.

[2] Docobo, J.A., Griffin, R.F., Campo, P.P, and Abushattal, A.A., Monthly Notices of the Royal Astronomical Society, 469 (1) (2017) 1096.

[3] Abushattal, A.A., Docobo, J.A., and Campo, P.P., The Astronomical Journal, 159 (1) (2019) 28.

[4] Alnaimat, S., Jameel, R., Abushattal, A., Al-Wardat, M., and Ahmed, M.H., In Arabic Conference of the Arab Union for Astronomy and Space Sciences and Tools for Decision Support, pages 8–20. Springer Nature Singapore, (2023).

[5] Abushattal, A.A., Alrawashdeh, A.A., and Kraishan, A.F. Communications of BAO, 69 (2) (2022) 251.

[6] Eggleton, P., "Evolutionary Processes in Binary and Multiple Stars", (Cambridge University Press, Cambridge, 2006).

[7] Abushattal, A.A., Al-Wardat, M.A., Horch, E.P., Geor-gakarakos, N., Al-Ameryeen, H.A., Abu-Alrob, E.M., and Hussein, A.M. Advances in Space Research, 73 (1) (2024) 1170.

[8] Docobo, J., Campo, P., and Abushattal, A., Iau commiss. Double Stars, 169 (1) (2018).

[9] Abushattal, A.A., Azzam, A.A.A., Al-Wardat, M.A., Widyan, H., Mardini, M., Taani, A., and Talafha, M., In Arabic Conference of the Arab Union for Astronomy and Space Sciences and Tools for Decision Support, pages 112– –130. Springer Nature Singapore, (2023).

[10] Hussein, A.M., Al-Wardat, M.A., Abushattal, A., Widyan, H.S., Abu-Alrob, E.M., Malkov, O., and Barstow, M.A., The Astronomical Journal, 163 (4) (2022) 182.

[11] Abushattal, A.A., The modeling of the physical and dynamical properties of spectroscopic binaries with an orbit, PhD thesis, Universidade de Santiago de Compostela, (2017).

[12] Alnaimat, S., Jameel, R., Abushattal, A., and Al-Wardat, M., In Proceedings of the 14th Arabic Conference of the Arab Union for Astronomy and Space Sciences (AUASS-CONF23), Sharjah, United Arab Emirates, 13–16 November (2023), Springer Nature, 420 (2025) 8.

[13] Abushattal, A.A., Al-Wardat, M.A., Taani, A.A., Khassawneh, A.M., and Al-Naimiy, H.M., Journal of Physics: Conference Series, 1258 (2019) 012018.

[14] Algnamat, B.S., Abushattal, A.A., Kraishan, A.F., and Alnaimat, M.S., Communications of BAO, 69 (2) (2022) 223.

[15] Alameryeen, H.A., Abushattal, A.A., and Kraishan, A.F., Communications of BAO, 69 (2) (2022) 242.

[16] Abushattal, A.A., Kraishan, A.F., and Alshamaseen, O.S., Communications of BAO, 69 (2) (2022) 235.

[17] Yousef, Z.T., Annuar, A., Hussein, A.M., Al-Naimiy, H., Al-Wardat, M., Abdul Hamid, N.S., and Talafha, M.F., Research in Astronomy and Astrophysics, 21 (5) (2021) 114.

[18] Al-Wardat, M.A., Bulletin of the Special Astrophysics Observatory, 55 (2003) 18.

[19] Al-Wardat, M.A., Astronomische Nachrichten, 328 (2007) 63.

[20] Masda, S.G., Al-Wardat, M.A., Neuhäuser, R., and Al-Naimiy, H.M., Research in Astronomy and Astrophysics, 16 (2016) 112.

[21] Abu-Alrob, E.M., Hussein, A.M., and Al-Wardat, M.A., The Astronomical Journal, 165 (6) (2023) 221.

[22] Masda, S.G., Al-Wardat, M.A., and Pathan, J.M., Journal of Astrophysics and Astronomy, 39 (5) (2018) 58.

[23] Al-Wardat, M.A., Docobo, J.A., Abushattal, A.A., and Campo, P.P., Astrophysical Bulletin, 72 (2017) 24.

[24] Al-Tawalbeh, Y.M., Hussein, A.M., Taani, A.A., Abushattal, A.A., Yusuf, N.A., Mardini, M.K., Suleiman, F.A., Al-Naimiy, H.M., Khasawneh, A.M., and Al-Wardat, M.A., Astrophysical Bulletin, 76 (2021) 71.

[25] Masda, S.G., Khan, A.R., and Pathan, J.M., American Institute of Physics Conference Series, 2335 (2021) 090002.

[26] Masda, S., New Astronomy, 111 (2024) 102244.

[27] ESA, "The Hipparcos and Tycho Catalogues", (ESA, 1997).

[28] SIMBAD, Simbad astronomical database, CDS Strasbourg.

[29] INF4, Fourth catalog of interferometric measurements of binary stars.

[30] Tokovinin, A., The Astrophysical Journal Supplement Series, 235 (1) (2018) 6.

[31] The g-tomo scientific data application (SDA), Explore Project.

[32] Cutri, R.M., Skrutskie, M.F., van Dyk, S., Beichman, C.A., Carpenter, J.M., Chester, T., Cambresy, L., Evans, T., Fowler, J., Gizis, J., Howard, E., Huchra, J., Jarrett, T., Kopan, E.L., Kirkpatrick, J.D., Light, R.M., Marsh, K.A., McCallon, H., Schneider, R., Stiening, R., Sykes, M., Weinberg, M., Wheaton, W.A., Wheelock, S., and Zacarias, N., VizieR Online Data Catalog, II/246 (2003).

[33] ESA (ed.), "The Hipparcos and Tycho Catalogues", ESA Special Publication, 1200 (1997).

[34] Sterken, C. (ed.), Astronomical Society of the Pacific Conference Series, 364 (2007).

[35] Al-Wardat, M.A., Astrophysical Bulletin, 69 (2014) 454.

[36] Al-Wardat, M.A., El-Mahameed, M.H., Yusuf, N.A., Khasawneh, A.M., and Masda, S.G., Research in Astronomy and Astrophysics, 16 (2016) 166.

[37] Al-Wardat, M.A., Bulletin of the Special Astrophysics Observatory, 53 (2002) 51.

[38] Al-Wardat, M.A., Astronomische Nachrichten, 330 (2009) 385.

[39] Al-Wardat, M.A., Balega, Y.Y., Leushin, V.V., Zuchkov, R.Y., Abujbha, R.M., Al-Waqfi, K.S., and Masda, S., Astrophysical Bulletin, 69 (2014) 198.

[40] Lang, K.R., "Astrophysical Data I: Planets and Stars", (Springer-Verlag, Berlin Heidelberg New York, 1992).

[41] Gray, D.F., "The Observation and Analysis of Stellar Photospheres", 4th ed., (Cambridge University Press, 2021).

[42] Al-Wardat, M.A., Hussein, A.M., Al-Naimiy, H.M., and Barstow, M.A., Publications of the Astronomical Society of Australia, 38 (2021) e002.

[43] Al-Wardat, M.A., Abu-Alrob, E., Hussein, A.M., Mardini, M.K., Taani, A.A., Widyan, H.S., Yousef, Z.T., Al-Naimiy, H.M., and Yusuf, N.A., Research in Astronomy and Astrophysics, 21 (7) (2021) 161.

[44] Tokovinin, A., Mason, B.D., Hartkopf, W.I., Mendez, R.A., and Horch, E.P., The Astronomical Journal, 151 (2016) 153.

[45] Washington Double Star Catalog, The sixth catalog of orbits of visual binary stars.

[46] Gaia Collaboration, VizieR Online Data Catalog, I/355 (2022).

[47] Fabricius, C., Høg, E., Makarov, V.V., Mason, B.D., Wycoff, G.L., and Urban, S.E., Astronomy and Astrophysics, 384 (2002) 180.

[48] Tokovinin, A., Mason, B.D., and Hartkopf, W.I., The Astronomical Journal, 139 (2010) 743.

[49] Tokovinin, A., Mason, B.D., and Hartkopf, W.I., The Astronomical Journal, 147 (5) (2014) 123.

[50] Tokovinin, A., Mason, B.D., Hartkopf, W.I., Mendez, R.A., and Horch, E.P., The Astronomical Journal, 150 (2015) 50.

[51] Girardi, L., Bressan, A., Bertelli, G., and Chiosi, C., Astronomy and Astrophysics Supplement Series, 141 (2000) 371.

[52] Miglio, A. and Montalbán, J., Astronomy and Astrophysics, 441 (2) (2005) 615.

[53] Girardi, L., Bressan, A., Bertelli, G., and Chiosi, C., VizieR Online Data Catalog, 414 (2000) 10371.

[54] Mason, B.D., Hartkopf, W.I., and Tokovinin, A., The Astronomical Journal, 140 (3) (2010) 735.

[55] Szebehely, V., Celestial Mechanics, 34 (1984) 49.

[56] Cockell, C.S. et al., Astrobiology, 16 (1) (2016) 89.

[57] Holman, M.J. and Wiegert, P.A., The Astronomical Journal, 117 (1) (1999) 621.

[58] Kopparapu, R.K., Ramirez, R., Kasting, J.F., Eymet, V., Robinson, T.D., Mahadevan, S., Terrien, R.C., Domagal-Goldman, S., Meadows, V., and Deshpande, R., The Astrophysical Journal, 770 (1) (2013) 82.